Sensitivity of photonic crystal fiber modes to temperature, strain and external refractive index

Chengkun Chen[1*], Albane Laronche[1], Géraud Bouwmans[2], Laurent Bigot[2], Yves Quiquempois[2], and Jacques Albert[1]

[1]*Department of Electronics, Carleton University, 1125 Colonel By Drive, Ottawa, Canada, K1S 5B6*
[2]*Université des Sciences et Technologies de Lille-CNRS, Laboratoire de Physique des Lasers, Atomes et Molécules, IRCICA, 59658 Villeneuve d'Ascq Cedex, France*
Corresponding author: chengkun.chen@gmail.com

Abstract: Several strong narrowband resonances are observed in the transmission spectra of fiber Bragg gratings photo-written in photonic crystal fiber that has a refractive index-neutral germanium/fluorine co-doped core. Experimental results for the strain, temperature and refractive index sensitivities of these mode resonances are reported and compared to those of conventional single mode fiber. In particular, we identify three kinds of resonances whose relative sensitivities to strain, temperature and refractive index are markedly different and present numerical simulations to explain these properties. Potential multiparameter optical sensor applications of these mode resonances are briefly discussed.

©2008 Optical Society of America

OCIS codes: (050.2770) Gratings; (060.2370) Fiber optics sensors; (060.5295) Photonic crystal fibers; (060.3735) Fiber Bragg gratings.

References and links

1. J. C. Knight, T. A. Birks, P. St. J. Russell, and D. M. Atkin, "All-silica single-mode optical fiber with photonic crystal cladding," Opt. Lett. **21**, 1547-1549 (1996).
2. P. Russell, "Photonic crystal fibers," Science **299**, 358–362 (2003).
3. J. C. Flanagan, R. Amezcua-Correa, F. Poletti, J.R. Hayes, N.G.R. Broderick, and D. J. Richardson, "Parasitic modes in large mode area microstructured fibers," in Optical Fiber Communication Conference, Technical Digest (Optical Society of America, 2007), paper OML4.
4. B. J. Eggleton, P. S. Westbrook, R. S. Windeler, S. Spalter, and T. A. Strasser, "Grating resonances in airsilica microstructured optical fibers," Opt. Lett. **24**, 1460-1462 (1999).
5. V. Beugin, L. Bigot, P. May, M. Lancry, Y. Quiquempois, M. Douay, G. Melin, A. Fleureau, S. Lempereur, and L. Gasca, "Efficient Bragg gratings in phosphosilicate and germanosilicate photonic crystal fiber," Appl. Opt. **45**, 8186-8193 (2006).
6. N. Groothoff, J. Canning, E. Buckley, K. Lyttikainen, and J. Zagari, "Bragg gratings in air-silica structured fibers," Opt. Lett. **28**, 233-235 (2003).
7. C. Chen and J. Albert, "Strain-optic coefficients of the individual cladding modes of a single mode fiber: theory and experiment," Electron. Lett. **42**, 1027-1028 (2006).
8. C. F. Chan, C. Chen, A. Jafari, A. Laronche, D. J. Thomson and J. Albert, "Optical fiber refractometer using narrowband cladding mode resonance shifts," Appl. Opt. **46**, 1142-1149 (2007).
9. O. Frazão, L. A. Ferreira, F. M. Araújo, and J. L. Santos, "Applications of fiber optic grating technology to multi-parameter measurement," Fiber Integrated Opt. **24**, 227 – 244 (2005).
10. G. D. Marshall, D. J. Kan, A. A. Asatryan, L. C. Botten, and M. J. Withford, "Transverse coupling to the core of a photonic crystal fiber: the photo-inscription of gratings," Opt. Express **15**, 7876-7887 (2007).
11. B. J. Eggleton, P. S. Westbrook, C. A. White, C. Kerbage, R. S. Windeler, and G. L. Burdge, "Cladding-mode-resonances in air–silica microstructure optical fibers," J. Lightwave Technol. **18**, 1084–1100 (2000).
12. C. Chen, L. Xiong, C. Caucheteur, P. Mégret and J. Albert, "Differential strain sensitivity of higher order cladding modes in weakly tilted fiber Bragg gratings," Proc. SPIE **6379**, 63790E1-7 (2006).
13. G. Laffont and P. Ferdinand, "Tilted short-period fiber-Bragg-grating-induced coupling to cladding modes for accurate refractometry," Meas. Sci. Technol. **12**, 765-770 (2001).
14. H. J. Patrick, "Analysis of the response of long period fiber gratings to external index of refraction," J. Lightwave Technol. **16**, 1606–1612 (1998).
15. A. Iadicicco, A. Cusano, A. Cutolo, R. Berini, and M. Giordano, "Thinned fiber Bragg gratings as high sensitivity refractive index sensor," IEEE Photon. Technol. Lett. **16**, 1149-1151 (2004).

16. M. C. P. Huy, G. Laffont, V. Dewynter, P. Ferdinand, L. Labonté, D. Pagnoux, P. Roy, W. Blanc, and B. Dussardier, "Tilted fiber Bragg grating photowritten in microstructured optical fiber for improved refractive index measurement," Opt. Express **14**, 10359-10370 (2006).

17. F. M. Cox, R. Lwin, M. C. J. Large, and C. M. B. Cordeiro, "Opening up optical fibres," Opt. Express **15**, 11843-11848 (2007).

18. I. M. White, and X. Fan, "On the performance quantification of resonant refractive index sensors," Opt. Express **16**, 1020-1028 (2008).

19. V. Bhatia, "Applications of long-period gratings to single and multi-parameter sensing," Opt. Express **4**, 457-466 (1999).

1. Introduction

Photonic crystal fiber (PCF) was first demonstrated in 1996 [1] and has been extensively explored for telecommunication and sensor applications [2]. In particular, solid core PCFs have rings of low refractive index inclusions, as air holes for example, along the radial direction, forming an equivalent inner cladding layer which has lower refractive index than the core and the pure silica outer cladding. In such structures, in addition to an endlessly single mode core mode and conventional cladding modes, there are cladding modes whose fields are confined only within the core and air-hole region [3,4]. Those unique characteristics of PCF cladding modes make them very attractive for sensor applications if the modes can be excited and measured in a controlled fashion. While all the modes will be sensitive to the temperature and strain perturbations, only some of the cladding modes will be sensitive to the surrounding media changes. We use photo-written fiber Bragg gratings (FBG) to selectively excite cladding modes in special PCFs that have a small fraction of the core co-doped with germanium [4,5] to increase their photosensitivity relative to undoped PCFs [6] and fluorine to keep the refractive index of the doped region close to the index of silica and prevent guidance in that layer.

In the work presented here, strong FBGs are written using a conventional phase mask technique and 193 nm ArF excimer laser irradiation. Even though the FBG fringes are not tilted with respect to the fiber axis, several strong cladding mode resonances are observed (in the transmission spectrum only) in addition to a 99.9% reflectivity core mode reflection. The strain, temperature and Surrounding Refractive Index (SRI) sensitivities of all these mode resonances will be presented here and compared with those of the core and cladding modes from tilted FBGs written in standard telecommunication fibers (Corning SMF-28 fiber) with the same laser irradiation set-up [7,8]. In standard fibers, the grating fringes must be tilted relative to the fiber axis in order to excite strong cladding mode resonances. Our experimental results for the relative sensitivity of the various modes will be supported by theoretical considerations and by simulations of the mode profiles of our fiber. Finally, we will discuss potential multiparameter optical fiber sensing applications based on the observed differential sensitivities of the resonances of these gratings. Of particular interest is the excitation of narrowband cladding mode resonances with the low temperature sensitivity of short period Bragg gratings and strong differential sensitivities to SRI and strain. While it is outside the scope of the present paper to compare this potential application to the wide variety of competing approaches for multiparameter sensing with fiber gratings [9], our PCF-FBGs present a certain number of unique features that may prove useful in certain applications.

2. Experimental conditions

The cross section of the experimental PCFs used in our work is shown in Fig. 1. The period between the air holes is 3.85 µm and the air hole diameter is approximately 1.75 µm. The core is roughly 6 µm in diameter with a 1.9 µm photosensitive region (3 wt% germanium and 0.9 wt% fluorine to reduce the index). The net index increase in the doped region is roughly 6×10^{-4} above the background pure silica. We used fluorine instead of boron to decrease the index of the germanium-doped region because it would have required too much boron to achieve the same reduction and resulted in higher losses. Note that the diameter and refractive index of the doped region of the core were designed to be small enough to prevent light from

being guided by this region (as confirmed by the results below). Guidance is thus totally caused by the holey cladding that contains 108 air holes. The PCFs are spliced with short pieces of SMF-28 to plug both ends before being hydrogen loaded at a pressure of 170 atm for 12 days and room temperature to enhance the photosensitivity. The SMF-28 fibers on both ends of the PCFs prevent the rapid out-diffusion of the hydrogen from the fiber due to the air-holes.
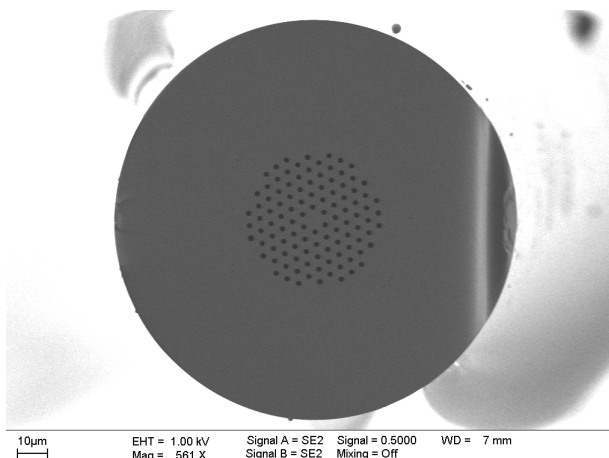

Fig. 1. The cross section of the photonic crystal fiber used in the experiment (outside fiber diameter = 125 µm). The doped core is not visible in these photographs.

The set-up for writing FBGs in PCFs is the same as for SMF-28 fiber, except that when writing in PCFs, during the alignment of the fiber at a low laser repetition rate (few Hz), the fiber is rotated around its axis until a maximum amount of light is transmitted across the air hole pattern to reach the fiber core [9]. Once this alignment is achieved, the fiber is fixed in place, about 50 µm from the phase mask and the writing as such is carried out (typically for 1-2 minutes at 100 Hz). We use 193 nm-wavelength ArF excimer laser light, with a fluence per pulse of approximately 100 mJ/cm^2. The phase mask has a period of 1106.5 nm and the length of the gratings written in the PCF is 1 cm. The FBG fabrication method used is completely standard (apart from the fiber rotation mentioned above), and yields usable gratings with great reliability. Furthermore, since we do not rely on absolute wavelength or power measurements in the proposed sensor implementations mentioned below (only relative values), minor variants in grating strength or wavelength have no impact on sensor performance. The measurement error for the individual resonance peaks is ±3 pm, the resolution of the JDSU SWS-OMNI-2 swept wavelength system that we used for measuring transmission spectra. For wavelength differences, the error becomes ±6 pm.

3. Results

Figure 2 shows the measured FBG transmission spectrum of a typical grating in our PCFs: in addition to the strong fundamental core mode (Bragg) resonance (that also appears in the reflection spectrum), there are several other narrowband non-reflective resonances with relatively large amplitude. These extra resonances can be attributed to a coupling of the forward propagating core mode to backward propagating cladding modes that do not propagate back all the way back to the measurement set-up.
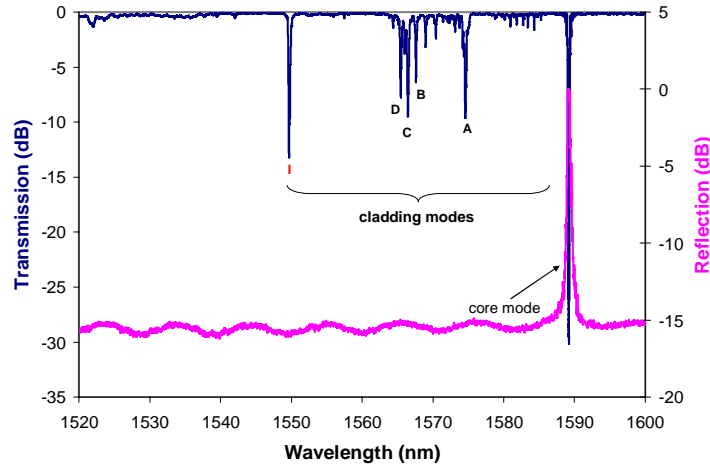
Fig. 2. The transmission and reflection spectra of a 1 cm-long FBG in PCF.

Table 1 gives quantitative details about those modes that have attenuations larger than -5 dB: their wavelength λ, amplitude, and relative distance from the Bragg resonance (λ_B - $\lambda_{cladding}$). The effective indices are obtained from the following standard formulas [7]: $n_{eff,core} = \lambda_B / 2\Lambda$ and $n^i_{eff,cladding} = \lambda^i_{cladding} / \Lambda - n^i_{eff,core}$, where Λ is half the mask period. Taking into account the precision of our measurement system (3 pm), the line width of the resonances (100 pm) and the uncertainty associated with the dispersion of the core effective index at wavelengths where the cladding resonances occur, we estimate that the effective indices of Table 1 are accurate to one part in 10^4.

The Bragg resonance transmission is larger than -30dB and its effective index (1.4363) is lower than that of silica at that wavelength (1.4438) thereby confirming that the core mode is not guided by the small doped section of the core. The strong cladding mode resonances seen in Fig. 2 are normally not happening in a well written FBG in conventional fiber unless a tilt angle is added [8]. We verified that the fringes generated by our writing set-up were not tilted by writing control gratings in SMF-28 fibers. Such strong cladding mode resonances are mainly caused by the fact that these cladding modes have strong fields in the core region [4] and that the grating is formed in a rather small portion of the core (the 1.9 µm diameter doped center), thereby enhancing the core to cladding modes couplings [11]. For practical purposes, only those modes which resonance amplitudes larger than 5 dB are investigated in the following for strain, temperature and surrounding refractive index (SRI) sensitivity.

Table 1. Summary of transmission resonances properties

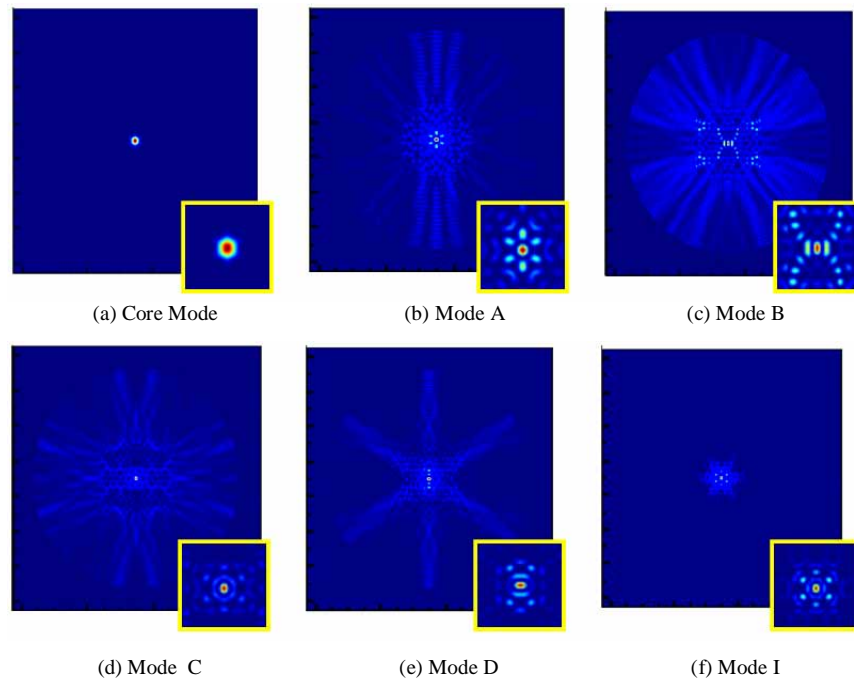| Mode	Resonance amplitude (dB)	λ (nm)	n_{eff} (exp)	n_{eff} (sim)	$\lambda_B - \lambda_{clad}$ (nm)	$d\lambda/dT$ (pm/^{o}C)	$d\lambda/d\varepsilon$ (pm/$\mu\varepsilon$)	Γ (sim)
Core	-30.13	1589.207	1.4363	1.4358		10.46	1.166	0.104
A	-9.67	1574.583	1.4096	1.4091	14.624	10.55	1.150	0.014
B	-6.37	1567.611	1.3969	1.3963	21.596	10.61	1.141	0.003
C	-9.49	1566.475	1.3949	1.3941	22.732	10.68	1.140	0.011
D	-7.78	1565.471	1.3931	1.3927	23.736	10.68	1.137	0.005
I	-13.23	1549.675	1.3643	1.3635	39.532	10.69	1.119	0.054

Fig. 3. The electric field intensities of the core mode and cladding modes, the insets show an enlarged view of the core area.

Before reporting on further experimental results, and in order to better understand the various modal sensitivities reported here, the modes of our PCF have been analyzed by using a mode solver based on the finite element method: Lumerical MODE Solutions from Lumerical Solutions Inc. The simulation window is 140 μm by 140 μm and perfectly matched layers are used as boundary conditions. The best match between the experimental effective index values and the simulation were obtained with a refractive index of 1.4514 in the doped region (the refractive index of the remainder of the glass is calculated from the Sellmeier equations for fused silica and is equal to 1.44383). The index of the doped region is significantly higher here than in the as-drawn fiber because of the relatively large index increase resulting from irradiating the hydrogen loaded doped silica. The simulated effective indices are given in Table 1 and the corresponding mode field distributions are shown in Fig. 3. It can be seen that fields of modes A to D extend all the way to the outer boundary while mode I is confined by the air hole structure that surrounds the core region. For each mode, the inset shows the detail of the mode structure in the vicinity of the core: all of these modes have strong field amplitude in the center of the fiber, where the doped region and hence the grating modulation are located. The confinement factor of each mode in the doped section (Γ in the Table), explains the relatively strong coupling between the core and cladding modes in the absence of tilt in the grating planes. For comparison, the confinement factors for the core mode and a typical cladding mode in standard fiber are 0.8 and 0.03 respectively, leading to poor overlap and weak coupling when no grating tilt is present.

Strain. The characterization of the strain sensitivity of individual resonances was carried out by stretching a grating rigidly bonded to two micrometric translation stages. Table 1 summarizes the results of these measurements, indicating small differences between the modes. These small differences can be monitored very precisely by using the Bragg mode resonance as a power and wavelength reference [7,8] and Fig.4 shows the result of such

relative measurements. The differential strain sensitivity of the different modes is seen to increase with the distance of the resonance from the Bragg peak, a behavior that was observed previously for the cladding mode resonances of TFBGs in conventional fibers (Corning SMF-28) [12].
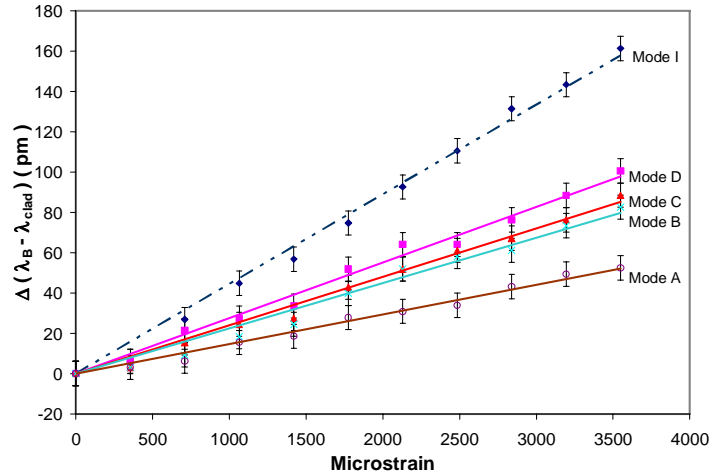

Fig. 4. The relative wavelength shifts of cladding mode resonances to the Bragg resonance of FBG due to axial strain perturbations.
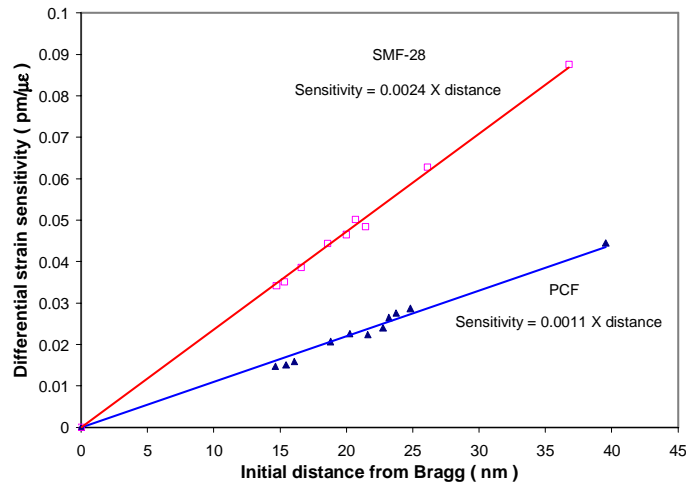

Fig. 5. The strain sensitivity differences of core and cladding modes in the PCF and SMF-28 fiber

For SMF-28 fiber, the strain sensitivity of the Bragg resonance is 10% smaller than that obtained here, i.e. 1.082 pm/με instead of 1.166 pm/με (for the core mode). However, when we plot the differential strain sensitivity of the cladding mode resonances relative to the Bragg resonance (i.e., the slopes of Fig. 4) as a function of the wavelength distance from Bragg resonance (Fig. 5) , we get the same linear dependence as was observed in SMF-28 fiber, but

with values consistently lower by a factor of about 2. This difference arises because of the higher refractive index contrast between the core and air-hole region in the PCF which confines more of the fields of the cladding modes in the fiber core area, especially in the doped region. This reduces the differential strain sensitivity between core and cladding modes compared with SMF-28 fiber where the core mode propagates in the germanium-doped region while the cladding modes have most of their energy localized in the silica cladding.
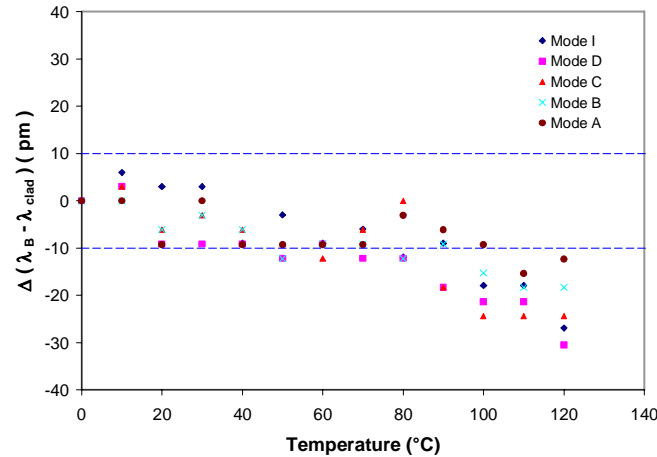

Fig. 6. The relative wavelength shifts of cladding mode resonances to the Bragg resonance of FBG due to temperature perturbations.

Temperature. Similarly to strain, the effect of temperature on our FBG-PCF resonances was measured from 0 °C to 120 °C in a temperature-controlled oven by tracking the individual resonance peak shifts as well as the differential temperature sensitivity (still relative to the Bragg resonance). The results are given in Table 1. For comparison, the temperature sensitivity of the Bragg resonance in SMF-28 fibers (9.579 pm/°C) is less than that obtained here (10.47 pm/°C). In terms of differential sensitivity, Fig. 6 shows the wavelength shifts of the cladding mode resonances relative to the Bragg resonance from 0 °C to 120 °C. The data shows a general downward trend (with slope of the order of -0.2 pm/°C, and superimposed random deviations not much greater than our estimated measurement accuracy), a similar behavior to what was observed in SMF-28 fibers ($\pm$ 10pm between –9 and +70°C [7]). Between 0 and 80°C, the relative cladding mode shifts vary between -12 and +8 pm which is equivalent to an uncertainty of ±500 $\mu\varepsilon$ for a strain measurement with mode I if the temperature is not known (i.e., for a temperature "blind" measurement in an environment where the temperature lies in that range).

Refractometry. Finally, another very widespread application of cladding mode-based fiber sensors is refractometry, since by definition the cladding mode resonances are sensitive to SRI. Out of the large body of literature on this topic, some representative examples include sensors based on tilted FBGs [8,13], long period gratings (LPG) [14], and cladding-reduced FBGs [15]. An additional possibility only available in PCFs consists of filling the air-holes with a gas or a liquid, thereby increasing the overlap between the perturbation and the cladding modes (and even between the core mode evanescent field in the air holes) [16]. The sensitivity of those sensors can be very high because of the strong field penetration in the medium filling the air-hole region, but it is somewhat difficult to get the material to be sensed to actually penetrate the holes [17]. In general, LPGs and TFBGs have different advantages
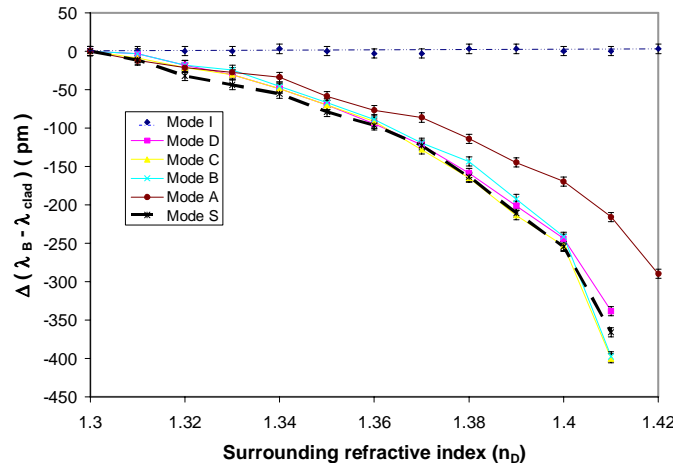
Fig. 7. The relative wavelength shifts of cladding mode resonances to the Bragg resonance of FBG with surrounding refractive index (n_D) changes.

and drawbacks but an important difference lies in the fact that while LPGs can be at least two orders of magnitude more sensitive than TFBGs, they are not necessarily more accurate because of a lower Q-factor (the wavelength of the resonance divided by width of the resonance) [18], and strong cross-sensitivities to multiple kinds of perturbations (strain, temperature, bending, etc..) [19]. Here we concentrate our efforts in measuring the SRI sensitivity of the cladding mode resonances to media located outside the fiber diameter. In the experiment, the grating was immersed in calibrated refractive index liquid oils from Cargille Corporation: the refractive indices listed (n_D) are the exact values at a wavelength of 589 nm (the supplier provides an equation to estimate the values of the refractive indices at the wavelengths we used but this equation has a listed uncertainty of 0.001). Fig. 7 shows the cladding resonance wavelength shifts due to surrounding refractive index changes. These absolute shifts are equivalent to differential wavelength shifts (relative to the Bragg resonance) since the Bragg resonance is totally immune to SRI. Therefore, apart from the ± 20 pm uncertainty noted above, using wavelength differences allows to perform refractometric measurements that are independent of temperature. An interesting feature of Fig. 7 is the fact that mode I is also insensitive to SRI changes, as expected from the simulated mode profile of Fig. 3 (SRI independent modes were previously identified in [4]). Other cladding mode resonances behave as usual and their sensitivity increases when the cladding mode approaches its cutoff (i.e. effective index = SRI). For comparison, Fig. 7 also shows a cladding mode (mode S) response for a SMF-28 fiber. The resonance wavelength of mode S is located 23.8 nm from the Bragg wavelength, the same distance as mode D in our PCF. It can be seen that the index sensitivity of mode D and mode S are almost the same, which means that $\partial n_{eff}/\partial n_{SRI}$ of the cladding mode involved in both fibers is almost the same even though the effective index and absolute wavelengths are different. The measurement range for SRI is similar for both types of fiber, from 1.3 to 1.42 but the great advantage of the PCF is that a single cladding mode can be followed over many nanometers without ambiguity from neighboring modes. In SMF-28 fibers the cladding modes are separated by 400-1000 pm, while here, as can be seen from Fig. 2 if a -5 dB threshold is used for mode finding, mode B can be unambiguously followed over a 5000 pm window and mode D for over 15000 pm. The best sensitivity reaches ~12 nm/RIU (RIU=refractive index units) in SRI ranges where each mode approaches cut-off. Given a detection system with a resolution of 6 pm (for the wavelength *difference* between the Bragg and the cladding mode used) this corresponds to a detection limit of 5×10^{-4} RIU.

4. Summary

In summary, strong FBGs are written in a germanium/fluorine co-doped core, hydrogen-loaded PCF with 193nm ArF excimer laser light and a phase mask. A limited number of strong cladding mode resonances are obtained with an un-tilted FBG, in contrast to conventional fibers where a large number of strong cladding mode resonances can be obtained, but only when the grating planes are tilted. The strain, temperature and refractive index sensitivities of core and cladding mode resonances in this PCF have been determined experimentally. In addition to the usual core and cladding modes, this PCF has a cladding mode whose optical field is confined by the air-hole region, making this mode insensitive to the surrounding refractive index changes, just like the core-guided mode. Like in conventional fibers, the cladding mode resonances in PCF show very small differential temperature sensitivity relative to the Bragg resonance, less than 0.2 pm/°C. Given this characteristic, making differential measurements of the wavelength of individual resonances with respect to the Bragg wavelength will be relatively independent of temperature. On the other hand, the differential strain sensitivity of the cladding mode resonances relative to the Bragg resonance increases linearly with the initial distance of each resonance from the Bragg resonance. This differential strain sensitivity of the cladding mode resonances in our PCF turns out to be a factor of 2 smaller than in SMF-28 fiber. We explain this difference by the larger confinement of the cladding modes studied in the core region of the PCF (due to the air-holes), which reduces the difference in the photo-elastic effect seen by the cladding modes, relative to the core modes. Finally, apart from the air hole confined mode (mode I) the refractive index differential sensitivities of the cladding modes behave exactly like the modes of conventional fiber: the wavelength shift per RIU converge to values around 10 nm/RIU as the modes approach cut-off in both types of fibers. The main advantage of the PCF short period gratings in sensing applications resides in the presence of the SRI-insensitive mode I, whose differential resonance shift can be used to sense axial strain independently of temperature and regardless of the material in which the sensor is placed, including liquids, epoxies or structural materials such as concrete. While the individual sensitivities of our sensor do not match the best values obtained with optimized single-parameter sensors, we feel that the multiparameter sensing capability, very low cross-sensitivity to temperature, and simple sensor construction is a distinct advantage.

Acknowledgement